

PAPER • OPEN ACCESS

Numerical construction of deformation field in converging channel

To cite this article: N A Damanhuri *et al* 2021 *J. Phys.: Conf. Ser.* **1988** 012023

View the [article online](#) for updates and enhancements.

A promotional banner for the 240th ECS Meeting. The banner features a colorful striped border at the top. On the left, the ECS logo is displayed in a green circle. To the right of the logo, the text reads: "240th ECS Meeting", "Digital Meeting, Oct 10-14, 2021", "We are going fully digital!", "Attendees register for free!", and "REGISTER NOW" in bold orange letters. On the right side of the banner, there is a photograph of a diverse group of people in a professional setting, with a man in a white shirt and tie clapping and smiling.

ECS **240th ECS Meeting**
Digital Meeting, Oct 10-14, 2021
We are going fully digital!
Attendees register for free!
REGISTER NOW

Numerical construction of deformation field in converging channel

N A Damanhuri¹, S Ayob¹ and I S Sabri¹

¹Centre for Mathematical Sciences, College of Computing and Applied Sciences, Universiti Malaysia Pahang, Lebuhraya Tun Razak, 26300 Gambang, Kuantan, Pahang, Malaysia

Email: noralisa@ump.edu.my

Abstract. This work proposes the computational method for the construction of the stress field in the deformation region in a converging channel. The stress components are assumed to satisfy Mohr-Coulomb yield criteria under plane strain condition. The governing equation for the model is the first-order partial differential equation, which is the stress equilibrium equations. The deformation region is made up of the union of adjacent elementary boundary value problem and solved numerically. The region is constructed by using Matlab, and it shows the formation of the two symmetrical deformation region at both upper and lower part of the converging channel. From the computation, we obtained the stress variables and the velocity distribution in the deformation region. The work rate for the corresponding velocity was calculated, then it is shown that the solutions are physically significant since the condition of the work rate is everywhere positive. This method is of great interest as it will bring about an increase in efficiency and hence improvement in industrial productivity, especially in designing granular flow device. The technique is also an alternative for the solution of the deformation problems as it is simple and more reliable.

1. Introduction

Granular materials can be found across a wide range of scales for example, in the kitchen, we have sugar, salt, cereals, in geophysics, we found sand, gravel, as well as, asteroids in astrophysics, [1]. Storage, handling, and processing of granular materials are procedures required in numerous industries and are of interest to various branches of science and technology such as physics, chemistry, mechanics, agriculture, and engineering. The agriculture and food industry are, next to chemical, power, and pharmaceutical industries, the largest producers and users of granular materials.

It is not easy to figure out the micro-mechanical behaviour of granular flow, they exhibit complex behaviour. They cannot be classified as the properties of solids, liquid or gases. The equipment for storage and processing of granular materials should meet two necessary conditions, which are predictable and safe operations and high quality of finished products. A precise knowledge of how they behave under these circumstances is essential for the efficient design and application of related industries. Their behaviour is like a new form state besides those three properties. The mathematical modelling for these materials is very complex due to their mechanical behaviour. For example, when one adds wheat, sugar, grains, cement, or sand and gravels, the fact that all these materials need to be transported and stored, the importance of granular materials become self-evident. Granular materials usually stored in hoppers or bins. Some agricultural hoppers that contain, for example, grains, can measure up to 20m in diameter and 60m height. The predictions of the stress distributions and the flow patterns throughout the hopper are exceptionally very important. The stresses can be so significant, and



the flow pattern can be so complicated, which can cause the hoppers to collapse or destroyed. Although there are many industrial applications, this field still requires more accurate scientific analysis to control loss in production, extra labour and inefficient use of capital. In many situations, we need considerable improvement in the flow of granular materials.

The theory of granular flow is the most interesting and intensively developing fields of mechanics because of its wide area of applications, especially in manufacturing process. Extrusion is one of the most widely used in manufacturing process for making a wide range of products, especially in food manufacturing process [2]. Extrusion is the process of forcing the material to flow through the various shape of dies forming various shapes of the product as shown in figure 1. Food manufacturing industry use extrusion technology in the production of cereal-based food, pasta, pet foods, etc. [3].

In this paper, we applied the numerical solution method in [4] to construct the deformation region in the converging channel. The solution method is based on the double-slip and double-spin model given by [5-6]. The deformational response to loading is assumed to be planar and rigid-plastic and the flow occurs at each point in the deformation region of two simultaneous shears. The material flows through the channel from the original converging channel width $2H$ is to the width $2h$ at the exit.

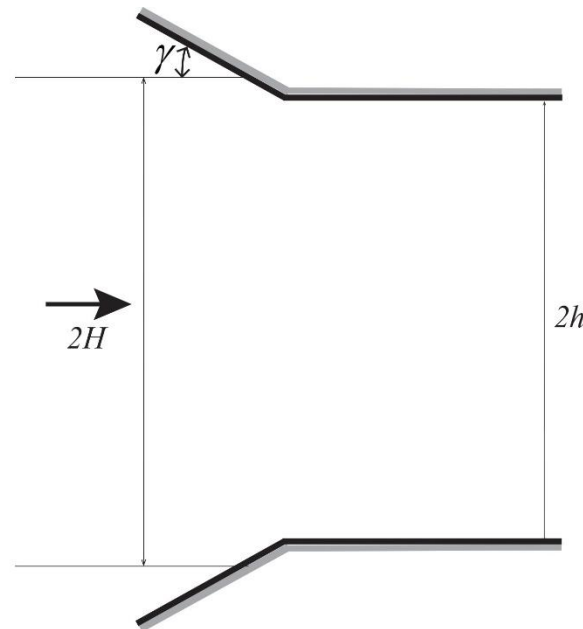


Figure 1. Flow through a converging channel.

2. The governing equation

The governing equations involved in this study are the equilibrium equations [7], given by

$$\frac{\partial \sigma_{11}}{\partial x} + \frac{\partial \sigma_{12}}{\partial y} = 0 \tag{1}$$

$$\tag{2}$$

$$\frac{\partial \sigma_{12}}{\partial x} + \frac{\partial \sigma_{22}}{\partial y} = 0$$

with Mohr Coulomb yield criterion

$$\tau = c - \sigma_n \tan \phi \tag{3}$$

where c and ϕ are material constants that represent cohesion and internal friction. From equation (1) and (2), we define the stress characteristic directions relative to the α - and β -characteristic lines respectively by

$$\frac{dy}{dx} = \tan[\psi \mp \left(\frac{\pi + 2\phi}{4}\right)] \tag{4}$$

The stress relations along the characteristics are,

$$\begin{aligned} \cos \phi \frac{\partial p}{\partial s_\alpha} + 2q_\alpha \frac{\partial \psi}{\partial s_\alpha} &= 0, \\ \cos \phi \frac{\partial p}{\partial s_\beta} - 2q_\beta \frac{\partial \psi}{\partial s_\beta} &= 0. \end{aligned}$$

Along the wedge, the coordinates $(x_n, y_n), (x_{n-1}, y_{n-1})$ and stress variables $(p_n, \psi_n), (p_{n-1}, \psi_{n-1})$ are known. Thus from equation (4), the approximated solution at a point x_{n+1}, y_{n+1} are given by

$$x_{n+1} = \frac{x_n \tan[\psi_\beta + \left(\frac{\pi + 2\phi}{4}\right)] - x_{n-1} \tan[\psi_\alpha - \left(\frac{\pi + 2\phi}{4}\right)] + y_{n-1} - y_n}{\tan[\psi_\beta + \left(\frac{\pi + 2\phi}{4}\right)] - \tan[\psi_\alpha - \left(\frac{\pi + 2\phi}{4}\right)]} \tag{5}$$

$$y_{n+1} = \frac{(x_n - x_{n-1}) \tan[\psi_\beta + \left(\frac{\pi + 2\phi}{4}\right)] \tan[\psi_\alpha - \left(\frac{\pi + 2\phi}{4}\right)] - y_{n-1} \tan[\psi_\alpha - \left(\frac{\pi + 2\phi}{4}\right)] - y_n \tan[\psi_\alpha - \left(\frac{\pi + 2\phi}{4}\right)]}{\tan[\psi_\beta + \left(\frac{\pi + 2\phi}{4}\right)] - \tan[\psi_\alpha - \left(\frac{\pi + 2\phi}{4}\right)]} \tag{6}$$

where

$$\psi_\alpha = \frac{1}{2}(\psi_{n-1} + \psi_{n+1}) \text{ along } \alpha\text{-characteristic} \tag{7}$$

$$\psi_\beta = \frac{1}{2}(\psi_n + \psi_{n+1}) \text{ along } \beta\text{-characteristic} \tag{8}$$

And the solution for stress variables p_{n+1} and ψ_{n+1} can be defined by,

$$\psi_{n+1} = \frac{(p_{n-1} + p_n) \cos \phi + 2q_\alpha \psi_{n-1} + 2q_\beta \psi_n}{2q_\alpha + 2q_\beta}, \tag{9}$$

$$p_{n+1} = \frac{p_{n-1} \cos \phi + 2q_\alpha (\psi_{n-1} - \psi_{n+1})}{\cos \phi}, \tag{10}$$

along α - and β - characteristic lines respectively, where

$$q_\alpha = \frac{1}{2}(p_{n-1} + p_{n+1}) \sin \phi + c \cos \phi \tag{11}$$

$$q_\beta = \frac{1}{2}(p_n + p_{n+1}) \sin \phi + c \cos \phi \tag{12}$$

3. The construction of deformation region

We assumed that there is no friction between the granular material and the wall, so that all characteristic lines meet the die face at $(\pi + 2\phi)/4$ at point A and B as in figure 2. In this case, the velocity and the stress fields do not vary with time and the parts of the material which are far from the die are assumed to be undeformed.

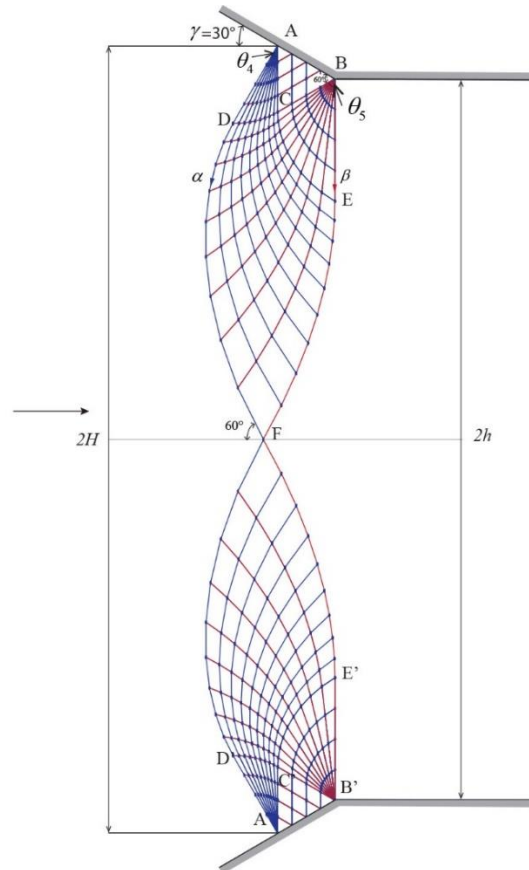


Figure 2. Deformation region in converging channel.

The punch surface AB of the container with semi angle $\gamma = 30^\circ$ is divided into $(n - 1)$ equal length segments and each point is labelled $(1,1), (2,1), \dots, (n, 1)$. The coordinates (x, y) and the stress variables, (p, ψ) of each point on the punch surface AB are known, then the stress characteristic field in the region ABC is obtained from equations (7) – (12) where the line AC is an α –characteristic line and line AB is the β –characteristic line. Both lines AC and BC are straight. Since the zone of plastically deforming material must extend through the channel, the point F lies on the centerline, so that it is common to the two plastic regions spreading symmetrically from the opposite side of the channel wall.

Then, we constructed two centered fan field regions ACD and BCE at two singular points A and B , respectively. Since the counter clockwise angle made by BE with the axis is $\frac{\pi}{4} + \frac{\phi}{2} + \theta_5 - \gamma$, from Hencky’s first theorem [8], the angles $DAC = \theta_4$ and $CBE = \theta_5$ must satisfy the relation

$$\theta_5 - \theta_4 = \gamma. \tag{13}$$

From the relation (13), let

$$\theta_4 = 30^\circ \tag{14}$$

as an initial guess. Therefore, we have

$$\theta_5 = \gamma + \theta_4 = 60^\circ. \tag{15}$$

From all known initials and stress variables, we constructed two centered fan region ACD and BCE similarly constructed by [9]. As a result, the intersection of two known characteristic lines, an α –characteristic line and the β –characteristic line at point C led to the determination of the stress field in the region $DCEF$.

Then, by using the equations (7) – (12), the stress distribution field in the region $DCEF$ is determined. The plastic field in the channel now fully constructed as shown in figure 2. The ψ distribution for the upper half of the channel is shown in figure 3. At point F , the value of ψ_F is equal to zero, and the characteristic line at point F must be inclined at 60° to the centerline.

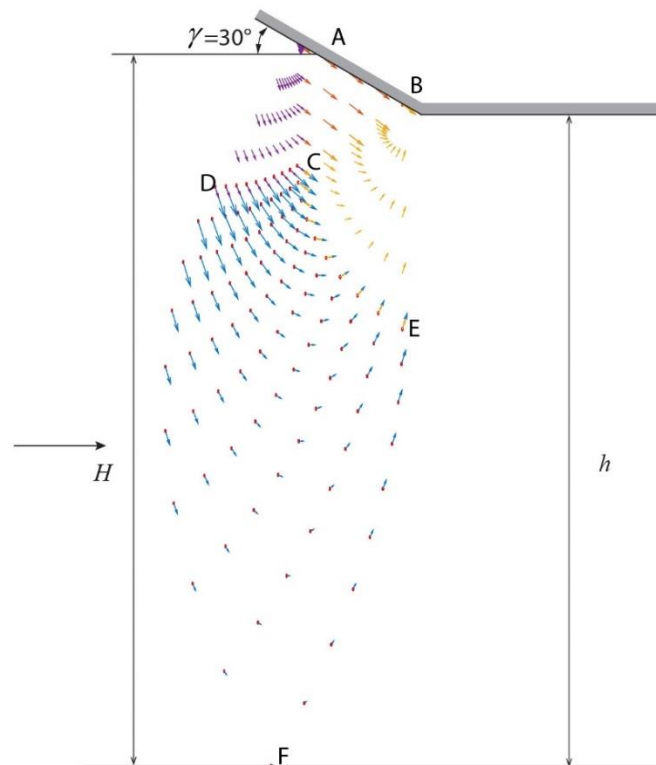


Figure 3. ψ distribution in the converging channel.

Since we have determined the network of the characteristic lines and the stress distribution in the converging channel, we now proceed to define the corresponding velocity distribution. We began our calculation by determining the velocity distribution for region $DCEF$. Since the left side of the material, ADF moves as a rigid body, the normal component of velocity, v_β is constant along the straight characteristic line AD . Similarly, the normal component of velocity, v_α along the straight characteristic line, BE is constant. The normal component velocity, v_β and v_α are known on the α –characteristic line ADF and β –characteristic line BEF respectively.

As an initial guess, at the characteristic line ADF ,

$$v_x = 1, \quad v_y = 0 \tag{16}$$

Since we have

$$v_\alpha \cos \phi = v_x \sin(\psi + \varepsilon) - v_y \cos(\psi + \varepsilon) \tag{17}$$

$$v_\beta \cos \phi = -v_x \sin(\psi - \varepsilon) + v_y \cos(\psi - \varepsilon) \tag{18}$$

then, we obtained

$$v_\alpha = \frac{1}{\cos \phi} \sin(\psi + \varepsilon) \tag{19}$$

$$v_\beta = -\frac{1}{\cos \phi} \sin(\psi - \varepsilon) \tag{20}$$

At the characteristic line BEF , we have

$$v_\alpha = \frac{1}{\cos \phi} \sin(\psi + \varepsilon) \tag{21}$$

$$v_\beta = 0 \tag{22}$$

From the relation (16) – (22) on the characteristic line DF and EF , we determined the velocity distribution in region $DCEF$, which gives the solution on CD and CE .

Now, by using the solution obtained on CD and CE together with the known components on AD and BE as the initial values, we determine the velocity distributions for both regions ADC and BCE . The solutions obtained on AC and BC line were then defined as the initial values to determine the velocity distribution in the region ABC . Since AC is a straight line, the velocity obtained in the region ABC is uniform and parallel to the die face. The velocity distribution in the plastic region for the upper half of the channel is shown in figure 4.

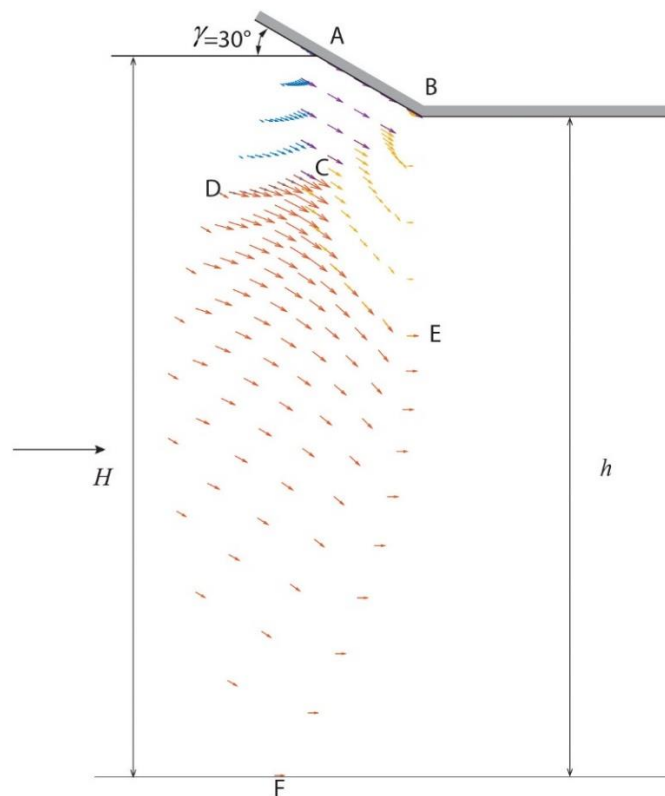


Figure 4. Velocity distribution in converging channel.

4. Results and Discussion

From the solution of the stress distribution field in the deformation region, we extended the numerical step to define the velocity distribution field by assuming that the characteristic lines for the stress coincide with the velocity characteristic lines. The numerical approximation to the solution has demonstrated some exciting features. By using the numerical method for the model, we have constructed the stress and velocity distribution field in the entire plastic region for the extrusion problem that has

not been previously solved for granular materials. It is shown that these solutions are physically significant since the condition that the work-rate be everywhere positive is satisfied.

In conclusion, the computational algorithm is useful to approximation to the solutions the deformation and flow of granular materials have and give beneficial insight into the flow of granular materials. A wide range of flow problems can now be successfully solved using the computer program. This algorithm can now be generalized to granular materials problems for many technical issues and structures, such as in transportation and storage.

Acknowledgement

We would like to thank the Universiti Malaysia Pahang for funding this research under UMP internal grant RDU190308.

References

- [1] Harris D 2014 A hyperbolic augmented elasto-plastic model for pressure-dependent yield *Acta Mechanica* **225**
- [2] Hambleton J P and Drescher A 2012 Approximate model for blunt objects indenting cohesive-frictional Materials
- [3] Gray D and Chinnaswamy R 1995 Chapter 13 - Role of extrusion in food processing (Food Processing ed Gaonkar A G) *Elsevier Science B.V.* pp 241-268
- [4] Ayob S and Damanhuri N A 2019 Numerical approximation of plane deformation for the indentation of granular material by a smooth rigid wedge punch *Universal Journal of Mechanical Engineering* **7** pp 166-171
- [5] Damanhuri N A M 2014 *The numerical approximation to solutions for the double-slip and double-spin model for the deformation and flow of granular materials* Ph.D. thesis The University of Manchester United Kingdom
- [6] Damanhuri N A and Ayob S 2017 A general numerical approximation of construction of axisymmetric ideal plastic plane deformation of a granular material *J. Phys. Conf. Series* **890** IOP Publishing p 012059
- [7] Hill J M and Selvadurai A P 2005 *Mathematics and Mechanics of Granular Materials* Springer pp 1-9
- [8] Hencky H 1933 The elastic behavior of vulcanized rubber *J Appl Mech* **1**(2), pp 45-53
- [9] Damanhuri N A M and Ayob S 2019 A general numerical approximation of the stress characteristic field at a singular point *AIP Conference Proceedings* **2184**(1) p 060030